Final Report to NOAA/AOML (Miami, Florida)

from

Pijush K. Kundu
Ocean Sciences Center
Nova University
Dania, Fl 33004

Analysis of Lagrangian Observations in the Caribbean Sea and the Gulf of Mexico

(Grant #04-78-Bol-19)

June 1980


NOAA
U.S. NATIONAL OCEANIC AND ATMOSPHERIC ADMINISTRATION
DEPARTMENT OF COMMERCE

I. INTRODUCTION

There have been several recent studies involving the tracking of a cluster of drifting buoys drogued at a suitable depth. Such a study can obviously establish the trajectory of the large scale ocean currents. But it can also determine the differential kinematic properties (DKP, such as divergence, vorticity, strain rate, etc.) of flow structures whose scales are of the order of the cluster size. One such study was that of Molinari and Kirwan (1975), who in particular examined whether the rate of change of potential vorticity

$$\frac{d}{dt}\left(\frac{\zeta+f}{D}\right) = \frac{d}{dt}(\zeta+f) + (\zeta+f)\nabla_H \cdot \underset{\sim}{V}$$

is nearly zero in the Yucatan Current, near the Mexican coast. (Here ζ is the vorticity, f is the Coriolis parameter, D is the depth of current, and $\nabla_H \cdot \underset{\sim}{V}$ is the horizontal divergence of current.) They found that, in several instances, the two terms on the right hand side of the potential vorticity equation have opposite signs, and nearly cancel each other. This simple balance was found to breakdown when the cluster was within about 50 km from the coast, presumably due to frictional effects.

A natural question that arises is the influence of friction on the movement of the cluster. In non-geophysical, laboratory flows the influence of turbulent friction is generally felt in boundary layers near walls. The flow away from walls has negligible turbulence since they cannot be maintained in the absence of shear. In geophysical flows the fluctuations can be continually created by baroclinic instabilities, thermal convections, etc. and therefore need not be confined to boundary layers only. The friction is expected to increase near coastal boundaries, however, because of the presence of the shear. It is observed that the longshore fluctuations

increase in magnitude near the coast (Kundu and Allen 1976), just like in laboratory flows.

Note that not all types of random fluctuations have the characteristics of "turbulence". A superposition of irrotational random waves going in different directions does not have the dispersive and dissipative characteristics of turbulence. A cluster of buoys in such a stationary homogeneous flow would drift apart and come together at various times, but the mean rate of increase of the enclosed area would be zero. The present note essentially examines whether there is a mean tendency for the area to increase. It will be found that, in most of the cases examined, there is a mean tendency for the area enclosed by a buoy cluster to increase with time.

Molinari and Kirwan (1975) describes how the DKP induced by scales of motion of the order of the cluster size are determined by a least square fitting technique. They attributed the scales of motion smaller than the cluster size as "turbulence". However, it is now suggested that this view is arbitrary, and misleading. The eddies that cause the gradual dispersion of the cluster most efficiently are, in fact, of the size of the cluster, just like the non-turbulent disturbances that cause only DKP without dispersion. The fact is, turbulent and nonturbulent motion cannot be separated simply by least square fitting. In geophysical circumstances the difference between them is fine and not at all well defined. It was seen by Molinari and Kirwan that the motion of the scale of the cluster size often satisfies the frictionless potential vorticity equation approximately. It will be seen here that the same motion also displays a gradual dispersion, a characteristic of turbulence.

2. REVIEW OF THEORY OF DISPERSION

(a) Dispersion of a single particle

The theory of dispersion of a particle from a point source was discussed in a fundamental work by G.I. Taylor (1921). Assuming one-dimensional fluctuations in a stationary and homogeneous turbulent medium, he showed that the mean square of the distance X travelled by a fluid particle in time t is given by

$$\frac{d}{dt}\left(\bar{X}^2\right) = 2\int_0^t R(\tau)\,d\tau \qquad (1)$$

where R is the Lagrangian auto-correlation function

$$R(\tau) = \overline{u(t)\,u(t+\tau)} \qquad (2)$$

Here the overbar denotes ensemble average; u(t) and u(t+ τ) are the fluctuating velocities of the same particle at times t and (t+τ) respectively. For small times (t<<$\mathcal{T}$, where $\mathcal{T}$ is the integral time scale), $R \approx \overline{u^2}$, and (1) shows that $\sqrt{\bar{X}^2} \sim t$. For t >>$\mathcal{T}$, equation (1) shows that $\sqrt{\bar{X}^2} \sim t^{1/2}$.

One can define an equivalent eddy coefficient such that a Fickian diffusion equation, of the form $\partial\theta/\partial t = k_{ij}\,\partial^2\theta/\partial x_i \partial x_j$ in two dimension, gives the same dispersion rate as (1). For homogeneous and stationary flow, it can be shown that (Batchelor 1949) the equivalent diffusivity in two dimensions is

$$k_{ij} = \frac{1}{2}\frac{d}{dt}\left(\overline{X_i X_j}\right) = \frac{1}{2}\int_0^t \left[R_{ij}(\tau)+R_{ji}(\tau)\right]d\tau \qquad (3)$$

where $R_{ij}(\tau) = \overline{u_i(t)\,u_j(t+\tau)}$. For isotropic flow in two-dimensions the above reduces to

$$k_{11} = k_{22} = \frac{1}{4}\frac{d\overline{r^2}}{dt} = \int_0^t R_{11}(\tau)\,d\tau = k \text{ say} \qquad (4)$$

where $r^2 = X^2 + Y^2$

(b) Relative Dispersion

Suppose two particles, in a cloud of fluid particles, are initially (t=0) separated by a vector $\underset{\sim}{\ell}_0$ (with components ξ_0, η_0, ζ_0) and that as a result of the turbulence the separation for any one trial is $\underset{\sim}{\ell}(t)$ (components $\xi(t)$, $\eta(t)$, $\zeta(t)$) at time t. Let $\delta u(t)$ be the x-component of the relative velocity of the two particles. Then the rate of increase of average distance between the two particles in the x-direction at time t is

$$\frac{d}{dt}\overline{\xi^2(t)} = 2\int_0^t \overline{\delta u(t)\,\delta u(t')}\,dt' \qquad (5)$$

This shows that $d(\overline{\xi^2})/dt \to t$ as $t \to 0$; it is also clear that $d(\overline{\xi^2})/dt \to 2\,d\overline{X^2}/dt$ as $t \to \infty$ since then the two particles wander independently. For intermediate values of ℓ_0 and t, $\overline{\xi^2}(t)$

lies between the Kolmogorof microscale and the large eddy structures, that is the inertial, locally isotropic range. Batchelor (1950) argues that then we must have

$$\frac{d\overline{\xi^2}}{dt} = f(t, \varepsilon) \tag{6}$$

where ε is the viscous dissipation rate. Equation (6) requires that

$$\overline{\xi^2} \sim \varepsilon t^3 \tag{7}$$

which can be rewritten as

$$\frac{d\overline{\xi^2}}{dt} \sim \varepsilon^{1/3} \overline{\xi^2}^{2/3} \tag{8}$$

Equation (8), which suggests that the eddy diffusivity is proportional to 4/3 power of the scale of the phenomenon, is known as Richardson's 4/3 law of eddy diffusivity. It has been found to be fairly good in the atmosphere (e.g., Richardson 1926) and in the ocean (Stommel 1949, Okubo 1971).

If there is no directional preference, an assumption already used in deriving (8), then the mean area $\bar{A}$ of a buoy cluster should be proportional to $\overline{\xi^2}$, and (8) can be rewritten as

$$\frac{d\bar{A}}{dt} \sim \varepsilon^{1/3} \bar{A}^{2/3} \tag{9}$$

If the flow has the dispersive characteristics of turbulence, then $\bar{A}$ must increase with time, possibly something like t^3 if Richardson's law is

approximately true. On the other hand, $d\bar{A}/dt$ would be zero if only frictionless wave motions were present; the buoys would then come closer and drift apart, without a mean tendency.

3. APPLICATION TO BUOY CLUSTER

During 1971-1976, several experiments were conducted by the group at AOML/NOAA, which involved the tracking of buoy clusters (3-5 buoys) in the Caribbean Sea and Gulf of Mexico. Some details of the experimental procedure are given in Molinari and Kirwan (1975). The data interval between consecutive position fixes is either 15 min. or 30 min. However, the position data appear to be dominated by random errors for periods less than 6h. Therefore, the data were first averaged to form hourly values, and then a running second-degree polynomial was fitted through 13 consecutive hourly positions. Evaluation of the polynomial at its midpoint, with a translation of the polynomial by 1 h, gives an hourly time series which can be regarded as a low-passed series with periods larger than 12 h. Drifter velocities were determined by center differencing in time.

In (9) the overbar denotes ensemble average, that is the average over experiments with identical initial conditions. Since this average cannot be determined in the present experiments, $\bar{A}$ at a certain t will be determined by passing a smooth curve through all A(t), as shown by the dotted line in the top left panel of Fig. 2.

Figure 1 shows the drifter trajectories of four legs of the 1971 western Caribbean Sea data, reproduced from Molinari and Kirwan (1975). Figure 2 shows the area of the buoy cluster versus time for each leg. It is seen that, in the mean, the area does increase with time in legs 1, 2 and 3, while it decreases slightly in leg 4. The increase is particularly rapid towards the end of leg 3, which can be explained as follows: The westward flow, impinging on the Mexico coast, monotonically converges and accelerates

northward, as evident in the speed plot of Fig. 1. With larger (relative) velocities, equation (5) shows that the rate of dispersion is larger. The rate of dispersion in other legs is smaller not only because the velocities are smaller, but also because the fluctuating velocities far from the coast presumably have less "frictional" or turbulence characteristics. If they are completely "wave-like", then the correlation function in (5) will have equal positive and negative areas, resulting in zero net dispersion at large times.

Figure 3 shows the areas for a few other cases, taken at different times in the Yucatan current and in the Gulf of Mexico. It is again seen that, in the mean, the area included by the buoy cluster increases in three out of four cases, although there is a great deal of fluctuation with time.

A plot of the eddy diffusion coefficient $d\bar{A}/dt$ versus $\bar{A}$ is shown in Figure 4. It is clear that the diffusivity increases with the scale of the phenomenon, but the data do not encompass a large enough range of $\bar{A}$ for testing the validity of the Richardson 4/3 law. (Presumably several decades of A values are needed for such a test.) Besides, the data from different regions are not expected to fall on the same line in Fig. 4, since ε is different (see Eq. 9). For example, the point with the highest $d\bar{A}/dt$ (~ 920 m^2/s) in Fig. 4 was found from the last part of Fig. 2, leg 3, where the cluster was near the coastal boundary layer and apparently had a larger ε .

4. CONCLUSIONS

An analysis of the Lagrangian position data of a cluster of buoys, consisting of 3-5 drifting buoys drogued at a depth of 20 m, shows that the included area generally increases in the mean, although there is a great deal of fluctuation with time. It seems that there are frictionless organized motions, superimposed on some "turbulence" that causes a gradual dispersion of the cluster with time. The tendency for dispersion increases near the coast, where the velocities and frictional mechanisms are larger.

It was found in Molinari and Kirwan (1975) that the frictionless potential vorticity equation had a qualitative validity in some cases, but the residual (much of which could presumably be attributed to frictional processes) can also be of the same order as the other terms in the equation. In all of the new data sets treated in the present work the residual was found to be non-negligible. It follows that the frictional terms are generally important in the vorticity balance, and an order of magnitude estimate confirms this. A typical eddy diffusivity for a scale length of $\Delta x \sim 5$km is found from Fig. 4 to be about $k \sim 200\ m^2/s$. Using $\zeta \sim 10^{-5}\ s^{-1}$ (Molinari and Kirwan 1975), we get the frictional term in the vorticity equation as $k\,\partial^2\zeta/\partial x^2 \sim 0.8 \times 10^{-10}\ s^{-2}$. The magnitude of the frictionless terms in the vorticity equation, namely $d(\zeta+f)/dt$ and $(\zeta+f)\,\nabla_H \cdot \underset{\sim}{V}$, were observed to be less than about $8 \times 10^{-10} s^{-2}$, with a typical magnitude something like $2 \times 10^{-10} s^{-2}$. The friction term thus seems to be somewhat less than, but of the order of, the frictionless terms of the vorticity equation. A frictionless balance may therefore be expected at places, but areas within 50 km of coasts should be dominated by friction, where $k > 1000\ m^2/s$ for similar spacial scales.

One idea suggested in Molinari and Kirwan is corrected here. It was suggested in that work that the relative distortion of the buoy cluster,

caused primarily by scales of motion of the size of the buoy cluster, could be separated from the "turbulent" field by using more than 3 buoys, and least square fitting in space. It is suggested in the present work that the turbulent field is not necessarily of a scale smaller than the cluster size. In fact, the turbulent eddies that are most effective in causing frictional as well as dispersive effects on a motion has a scale which is same as that of the phenomenon considered. Dispersive as well as other experiments in the ocean and the atmosphere indicate that the "equilibrium range", in which (9) is assumed to be valid, extends to hundreds of kilometers; in fact an upper limit beyond which (9) does not hold has not been detected. This makes sense, since geophysical flows have all ranges of eddy sizes, the largest of which are probably of the size of the ocean basins.

APPENDIX 1

Data Processing

Raw data of the buoy (x,y) coordinates at 15 min. intervals were supplied by NOAA/AOML, with a list of the known bad points. Many other bad points were detected by plotting the raw data series, and omitted. These and other existing gaps in the data series were patched by fitting second degree polynomials across the gap.

It was known that the position data were dominated by random measurement errors for periods less than 6h. However, these must also contain "turbulence," which is almost impossible to separate from random errors. The relative sizes of these two can in many cases be estimated from an autocorrelation plot. Since the measurement errors are incoherent, but turbulence has an integral time scale, one generally gets a plot with a sharp drop near the origin, followed by a much gentler decrease. This drop near the origin of the autocorrelation plot is a measure of the random error.

Figure 5 shows a typical autocorrelation plot of the v-component of velocity estimated from the 15 min. data. It is seen that the method fails because there is no gentle decrease due to the presence of turbulence. This is because the 15 min. data are so dominated by random errors that it completely overwhelms the turbulent components.

In order to eliminate the random errors, the data were low passed through a filter with a 12h half power point. The resulting series were seen to be fairly similar to the ones detained by fitting second degree polynominals through 13 consecutive hourly positions, as were done by Molinari and Kirwan (1975). In order to be consistent, we hose to continue with the polynomial fitting.

APPENDIX 2

Downstream Acceleration of the Yucatan Current

It was observed in Molinari and Kirwan (1975) that the Yucatan current accelerates rapidly downstream just before it enters the Yucatan Strait. It was not clear whether this was due to a "nozzle effect" because of decrease of flow area, or something else. I think it is not this nozzle effect — the presence of the island of Cuba has nothing to do with this. Two explanations are provided below.

(1) Without Rotation

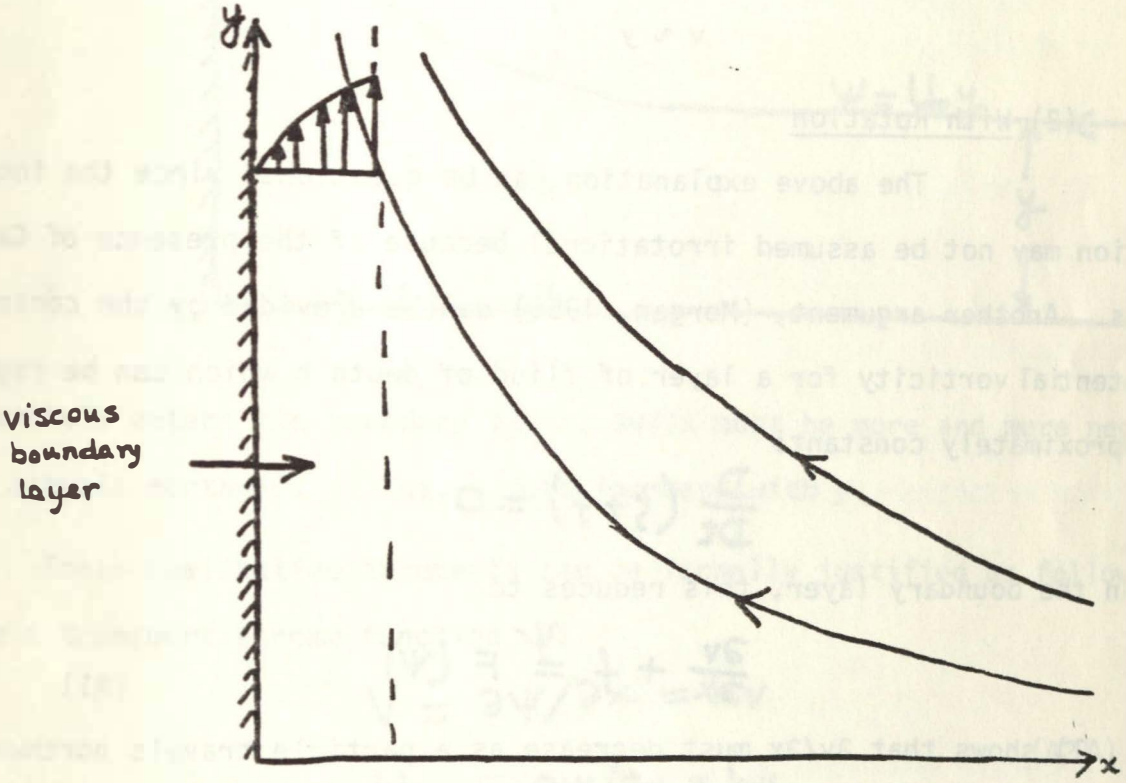

One explanation is that the acceleration is due to a continued convergence that occurs along a wall when an irrotational stream impinges upon it.

The irrotational flow given by the stream function

$$\Psi = kxy \qquad (k = \text{constant})$$

gives rise to

$$u = -kx$$

$$v = ky$$

Thus, v increases linearly along the wall. Even when one assumes a viscous boundary layer along the wall, it can be shown (e.g., Batchelor 1967, p285) that the similarity solutions within the boundary layer give

$$v \sim y$$

(2) With Rotation

The above explanation can be questioned since the interior solution may not be assumed irrotational because of the presence of Cariolis forces. Another argument, (Morgan, 1956) can be provided by the conservation of potential vorticity for a layer of fliud of depth h which can be regarded as approximately constant:

$$\frac{D}{Dt}(\zeta + f) = 0$$

Within the boundary layer, this reduces to

$$\frac{\partial v}{\partial x} + f = F(\Psi) \qquad (A1)$$

Eqn. (A1) shows that $\partial v/\partial x$ must decrease as a particle travels northwards into regions of larger $f\ (= f_0 + \beta y)$. Since $\partial v/\partial x$ is approximately zero when

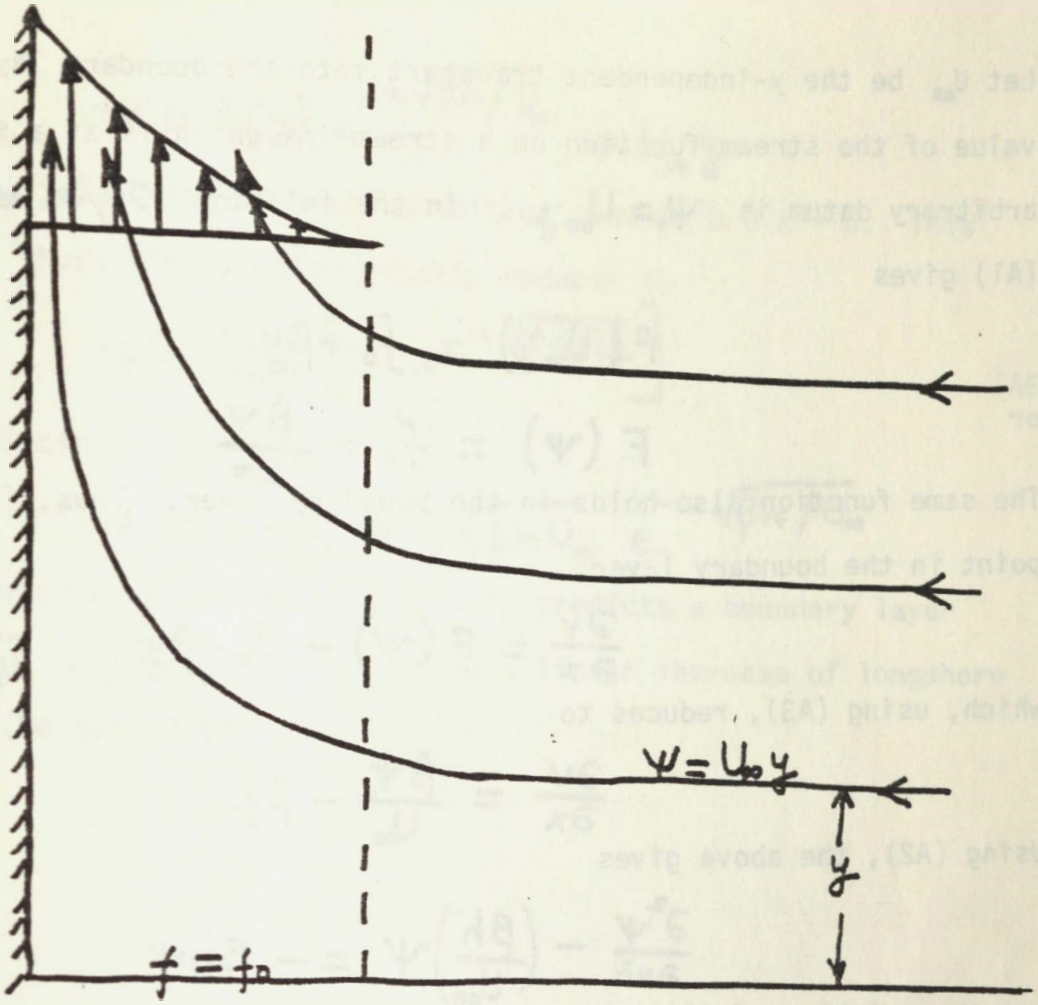

the particle enters the boundary layer, $\partial v/\partial x$ must be more and more negative as it travels northward. Thus, v must increase with y.

These qualitative arguments can be formally justified as follows. Define a transport stream function ψ:

$$V = \partial\psi/\partial x = hv$$
$$U = -\partial\psi/\partial y = hu \qquad \text{(A2)}$$

where

$$U = \int_0^h u\,dz$$

$$V = \int_0^h v\,dz$$

Let U_∞ be the y-independent transport into the boundary layer. Then the value of the stream function on a streamline which is at a distance y from an arbitrary datum is $\psi = U_\infty y$. In the interior $\partial v/\partial x \simeq 0$, and hence (A1) gives

$$F(U_\infty y) = f_0 + \beta y$$

or

$$F(\psi) = f_0 + \frac{\beta \psi}{U_\infty} \qquad \text{(A3)}$$

The same function also holds in the boundary layer. Thus, (A1) gives, for any point in the boundary layer,

$$\frac{\partial v}{\partial x} = F(\psi) - f_0 - \beta y$$

which, using (A3), reduces to

$$\frac{\partial v}{\partial x} = \frac{\beta \psi}{U_\infty} - \beta y$$

Using (A2), the above gives

$$\frac{\partial^2 \psi}{\partial x^2} - \left(\frac{\beta h}{U_\infty}\right)\psi = -\beta h \psi \qquad \text{(A4)}$$

Let the solution of (A4) be

$$\psi = \psi^c + \psi^p$$

The particular integral ψ^p, which satisfies the entire equation, is obviously linear in y. Letting $\psi^p = Ky$, a substitution into (A4) gives $K = U_\infty$. Thus

$$\psi^p = U_\infty y$$

The complementary function satisfies the homogeneous equation

$$\frac{\partial^2 \psi^c}{\partial x^2} - \frac{\beta h}{U_\infty}\psi^c = 0$$

whose solution is

$$\psi^c = A(y)\, e^{-x\sqrt{\beta h / U_\infty}}$$

Thus, the total solution is

$$\psi = A(y)\, e^{-x\sqrt{\beta h/U_\infty}} + U_\infty y$$

To determine A(y), apply the boundary condition that $\psi = 0$ @ x = o. This gives $A = -U_\infty y$. Thus, the solution finally reduces to

$$\psi = U_\infty y \left[1 - e^{-x\sqrt{\beta h/U_\infty}}\right] \qquad \text{(A5)}$$

The longshore velocity is

$$v = \frac{1}{h}\psi_x = y\sqrt{\beta h U_\infty}\; e^{-x\sqrt{\beta h/U_\infty}}$$

Thus, the conservation of potential vorticity predicts a boundary layer of width $\sqrt{U_\infty/\beta h} = \sqrt{u_\infty/\beta}$, and a linear increase of longshore velocity with y (Morgan 1956).

LIST OF FIGURES

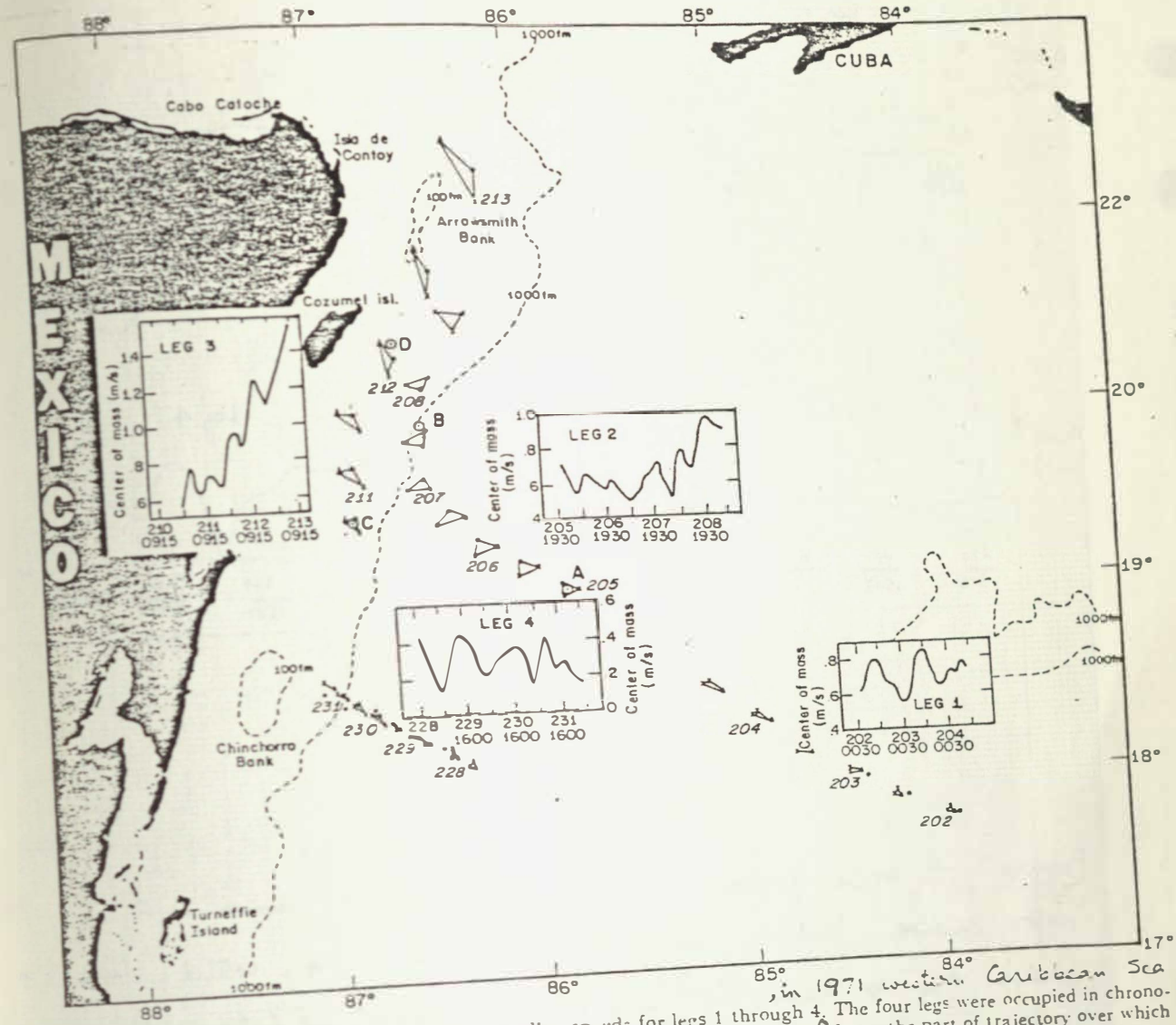

FIG. 1. Diagram of the drifter trajectories, including speeds for legs 1 through 4. The four legs were occupied in chronological order. The times are in Julian Day/Hour. The intervals (A, B) and (C, D) refer to the part of trajectory over which potential vorticity was conserved. ~~Figure 9~~ (Reproduced from Molinari and Kirwan 1975)

, in 1971 western Caribbean Sea data.

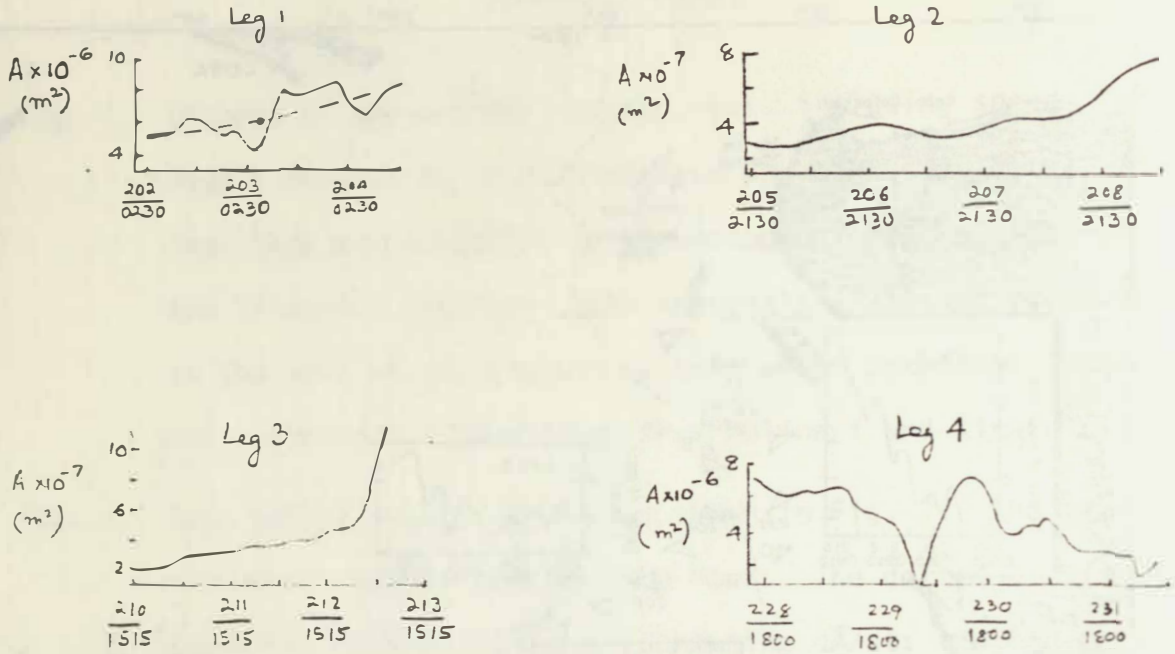

Figure 2 : Area versus time in four legs shown in Figure 1. The time axis shows Julian days and the hour. The dotted line in Leg 1 shows the 6 mean $\bar{A}$ used in computing $n\bar{A}/\partial t$; the mid-point of this dotted line is used in computing $\bar{A}$ in Eq. (9) (Redrawn from Molinari and Kirwan 1975).

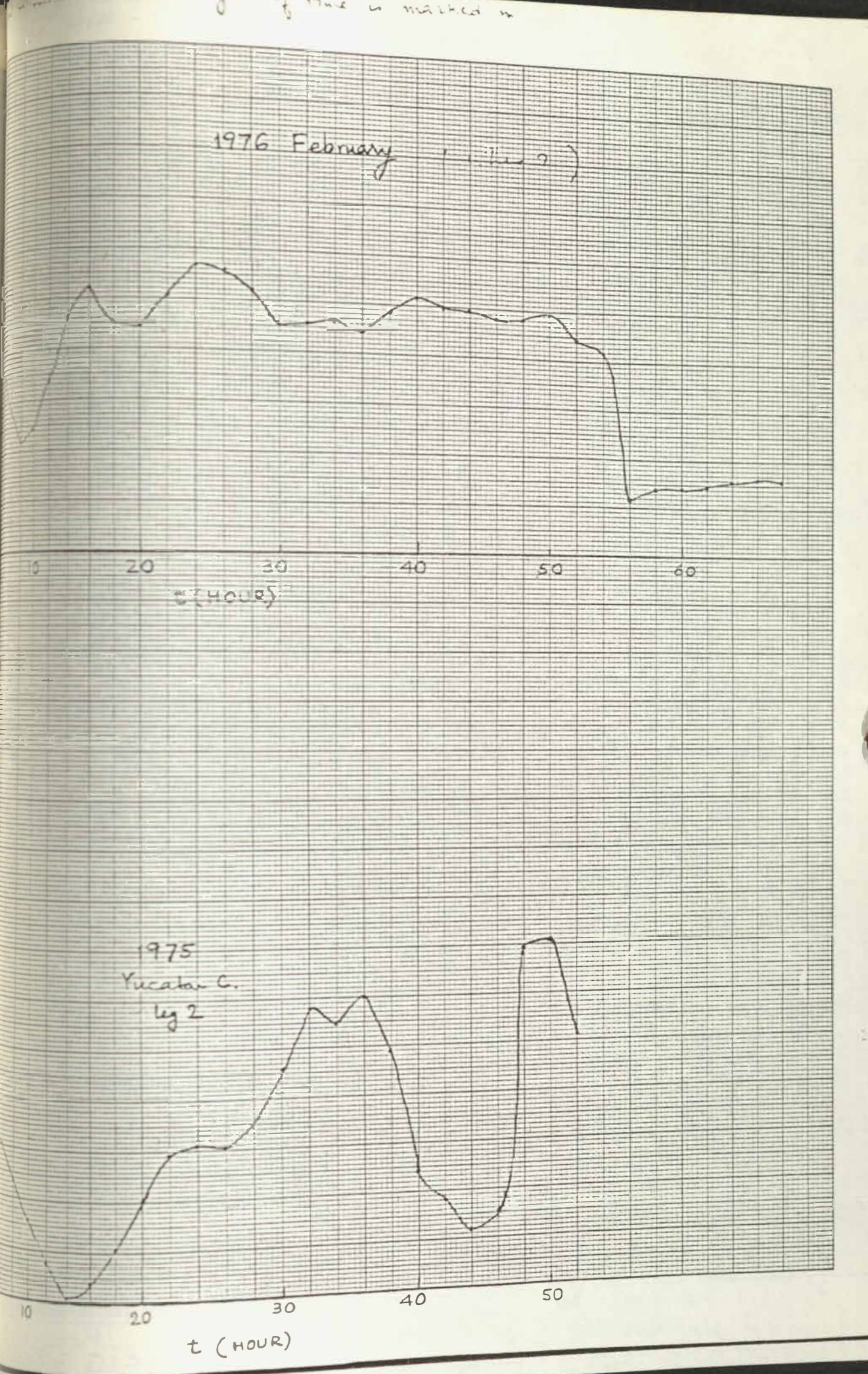
1976 February
10
20
30
40
50
60
t (HOUR)
1975
Yucatan C.
Lg 2
10
20
30
40
50
t (HOUR)

Fig 3. Area versus time in four experiments in the Gulf of Mexico Julian days and hours.

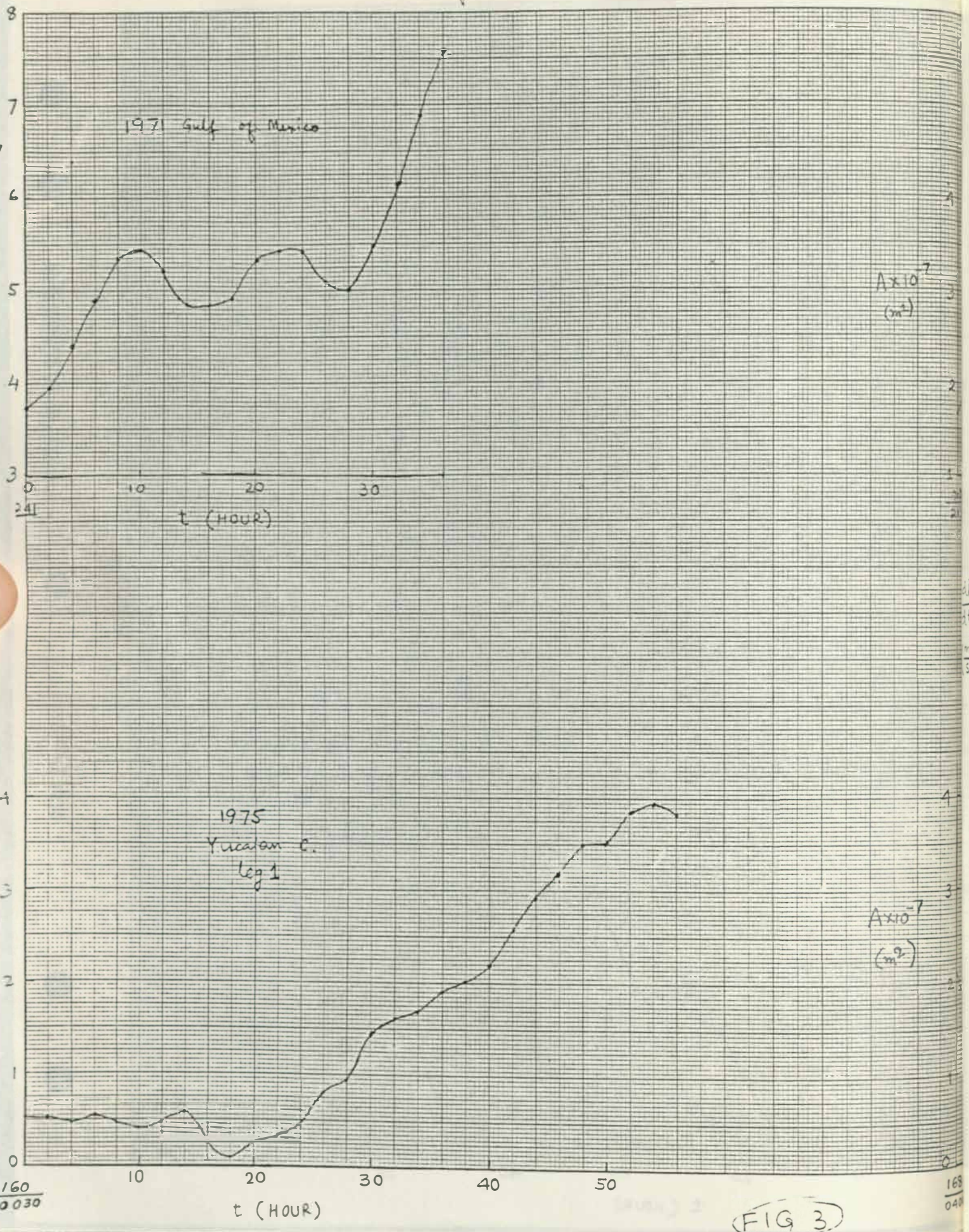

(FIG 3.)

Figure 4 Plot of $\frac{dA}{dt} \propto \frac{1}{\bar{A}^{3/2}}$. $\frac{dA}{dt}$ versus $\bar{A}$. The line indicates the slope

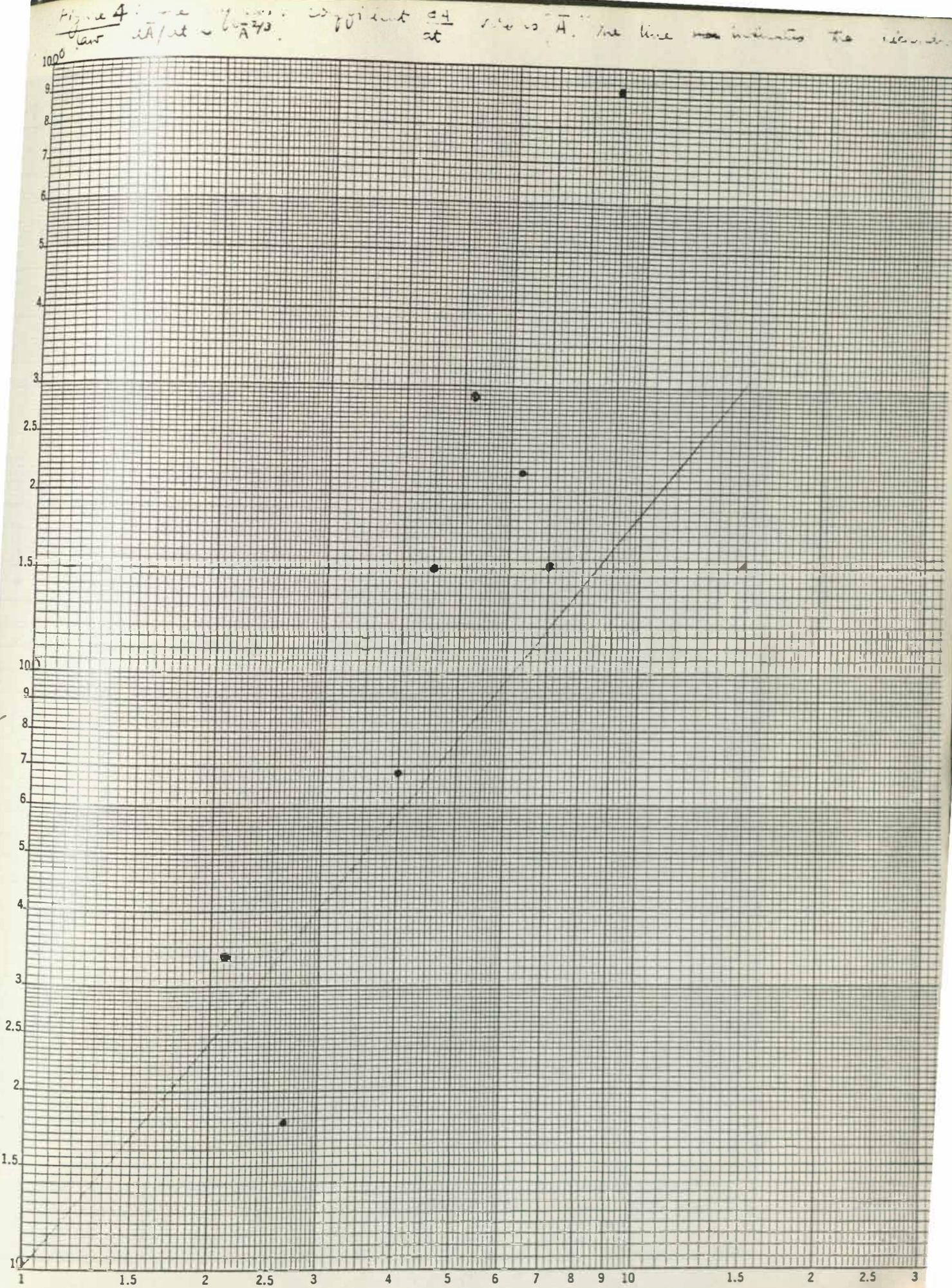

FIG 4

$\sqrt{A}$ (km)

REFERENCES

Batchelor, G.K., 1949: Diffusion in a field of homogeneous turbulence. I. Eulerian analysis. Aust. J. Sci. Res., Ser. A, 2, 437-450.

Batchelor, G.K., 1950: The application of the similarity theory of turbulence to atmospheric diffusion. Quart. J. Roy. Met. Soc., 76, 133-146.

Batchelor, G.K., 1967: An Introduction to Fluid Dynamics. Cambridge University Press.

Kundu, P.K., and J.S. Allen, 1976: Some three dimensional characteristics of low-frequency current fluctuations near the Oregon coast. J. Phys. Oceanogr., 6, 181-199.

Molinari, R., and A.D. Kirwan, 1975: Calculations of differential kinematic properties from Lagrangian observations in the western Caribbean Sea. J. Phys. Oceanogr., 5, 483-491.

Morgan, G.W., 1956: On the wind-driven ocean circulation. Tellus, 8, 301-320.

Okubo, A., 1971: Oceanic diffusion diagrams. Deep Sea Res., 18, 789-802.

Richardson, L., 1926: Atmospheric diffusion shown on a distance-neighbor graph. Proc. Roy. Soc., A110, 709-737.

Stommel, H., 1949: Horizontal diffusion due to oceanic turbulence. J. Mar. Res., 8, 199-225.

Taylor, G.I., 1921: Diffusion by continuous movements. Proc. London Math. Soc., Ser. 2, 20, 196-212.

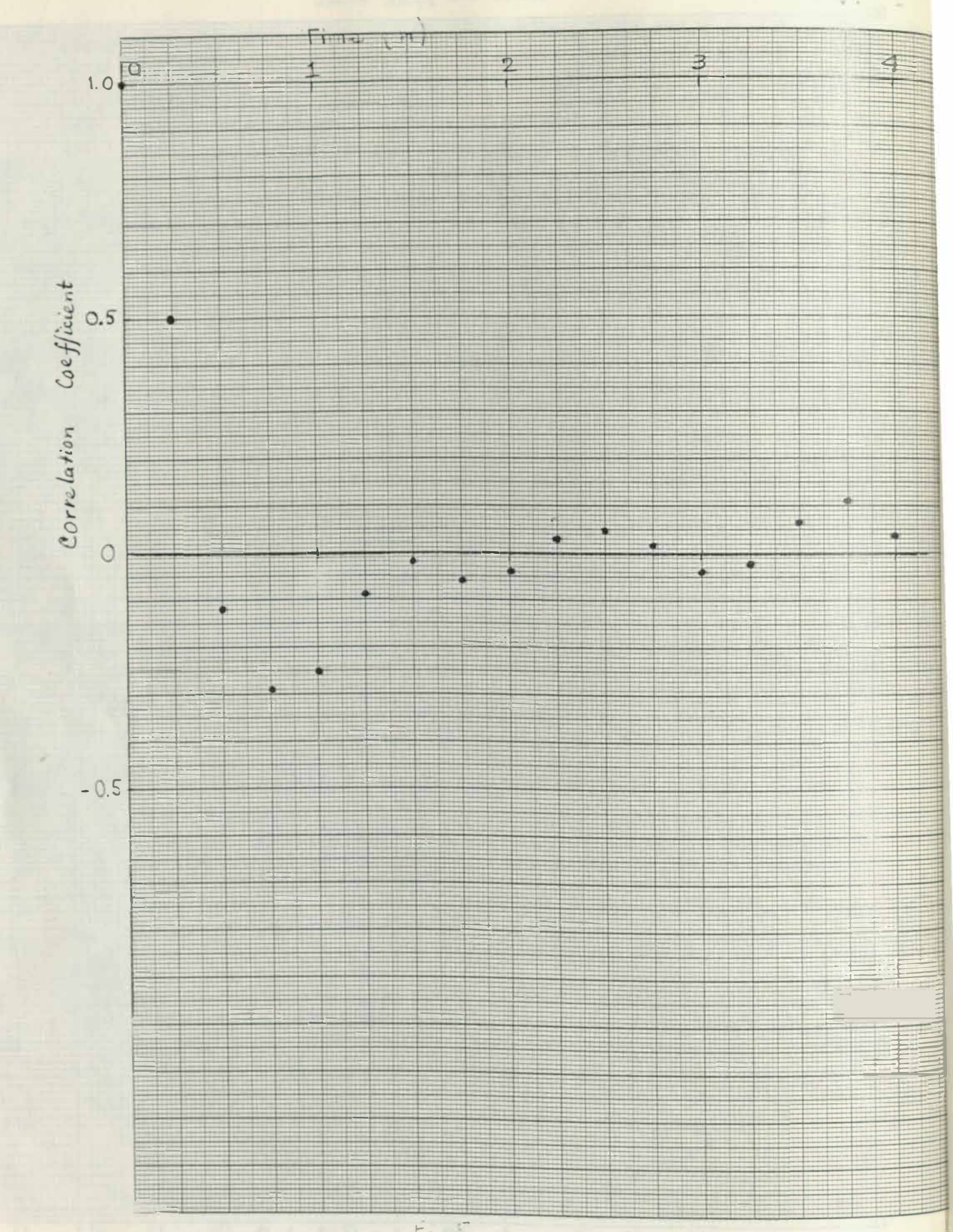
Correlation Coefficient
1.0
0.5
0
-0.5
0
1
2
3
4

REFERENCES

Batchelor, G.K., 1949: Diffusion in a field of homogeneous turbulence. I. Eulerian analysis. Aust. J. Sci. Res., Ser. A, 2, 437-450.

Batchelor, G.K., 1950: The application of the similarity theory of turbulence to atmospheric diffusion. Quart. J. Roy. Met. Soc., 76, 133-146.

Batchelor, G.K., 1967: An Introduction to Fluid Dynamics. Cambridge University Press.

Kundu, P.K., and J.S. Allen, 1976: Some three dimensional characteristics of low-frequency current fluctuations near the Oregon coast. J. Phys. Oceanogr., 6, 181-199.

Molinari, R., and A.D. Kirwan, 1975: Calculations of differential kinematic properties from Lagrangian observations in the western Caribbean Sea. J. Phys. Oceanogr., 5, 483-491.

Morgan, G.W., 1956: On the wind-driven ocean circulation. Tellus, 8, 301-320.

Okubo, A., 1971: Oceanic diffusion diagrams. Deep Sea Res., 18, 789-802.

Richardson, L., 1926: Atmospheric diffusion shown on a distance-neighbor graph. Proc. Roy. Soc., A110, 709-737.

Stommel, H., 1949: Horizontal diffusion due to oceanic turbulence. J. Mar. Res., 8, 199-225.

Taylor, G.I., 1921: Diffusion by continuous movements. Proc. London Math. Soc., Ser. 2, 20, 196-212.